JOURNAL OF MATERIALS SCIENCE 24 (1989) 1491–1495

Growth of zinc aluminate on the surfaces normal to the various crystal axes of an alumina single crystal

A. YAMAKAWA[‡], M. HASHIBA*, Y. NURISHI*
Department of Chemistry, Faculty of Engineering, Gifu University, Gifu 501-11, Japan
[‡] *Fuji Laboratory, Tokai Carbon Co., 394-1 Subashiri, Koyama-cho, Sunto-gun, Shizuoka 410-14, Japan*

The growth of a zinc aluminate layer on the surfaces normal to the various crystal axes of an alumina single crystal was determined and the microstructure of the reaction layer observed.

The microstructure of the thermally etched reaction layer showed in the grain structure that the reaction proceeded by the counter diffusion of cations as proposed by Wagner. The diffusion constant controlling the growth of the reaction layer was calculated. The diffusion constant showed a high activation energy of c.a. 400 kJ mol^{-1} which corresponded to the highest group of that of diffusion controlled zinc aluminate formation from zinc oxide and alumina of various physical natures. The high activation energy is also evidence of the counter diffusion of cations.

1. Introduction

It has already been reported by many investigators that the formation rate of $ZnAl_2O_4$ from ZnO and Al_2O_3 powders is controlled by diffusion [1–9].

The present authors [10–14] have reported that the growth rate of the $ZnAl_2O_4$ layer is affected by the physical nature of alumina such as electrofused dense alumina and also agglomerated fine alumina prepared by spray drying. The diffusion coefficient for the dense alumina system was smaller than that for the system including the agglomerates of fine alumina. The agglomerated alumina system [13, 15] resulted in a lower activation energy of the diffusion, i.e., about 200 kJ mol^{-1}, compared to that for the dense alumina systems, i.e., about 354 kJ mol^{-1} [10, 15].

It is valuable to examine the reaction on an alumina single crystal for the growth rate of the reaction layer, the diffusion constant and the activation energy of the diffusion as a standard to compare the values with those of polycrystalline alumina and of the agglomerated alumina systems.

Several authors have pointed out that the spinel layers of $ZnAl_2O_4$, $MgAl_2O_4$, $CoAl_2O_4$ and $NiAl_2O_4$ grown on an alumina single crystal [15–17] or dense polycrystalline alumina [18] were composed of two different layers identified with the differences of chemically etched states and the distribution of pores as a natural marker. The facts are explained by the counter diffusion mechanism of cations proposed by Wagner [20]. For $ZnAl_2O_4$ formation, the unidirectional diffusion mechanism of zinc oxide [1, 21] as assumed in the Jander model [22] or other improved model [22–25], and also the counter diffusion mechanism of cations [15] by Wagner [20] have been proposed. The physical natures of alumina powders should, however, be taken into consideration to apply these diffusion models for the growth of the $ZnAl_2O_4$ layer in the $ZnO–Al_2O_3$ system [14].

In this study the growth rate of $ZnAl_2O_4$ on the surfaces normal to the various crystal axes of an alumina single crystal were measured to obtain the diffusion coefficient and the activation energy of the diffusion. Concentration of the cations in the reaction layer was determined by an energy dispersive X-ray analyser. The thermal etching technique was applied to reveal the grain structure of the $ZnAl_2O_4$ layer. The diffusion mechanisms controlling the $ZnAl_2O_4$ formation on an alumina single crystal were discussed.

2. Experimental procedure

2.1. Materials

Alumina single crystals with surface normal to the various crystal axes were obtained from Shinkohsya (Tokyo, Japan). The purity of the crystal is above 99.99%. Zinc oxide powder was a guaranteed grade reagent from the Nakarai Chemical (Osaka, Japan).

2.2. Sample preparation and firing

The surface of alumina single crystals was coated with platinum vapour to act as a marker on the initial surface of the crystal. A thick zinc oxide suspension containing 0.2% of PVA as a binder was spread on the surface of alumina single crystal and then dried several times and fired for a fixed time and temperature.

2.3. Microstructural observation of the $ZnAl_2O_4$ layer

The fired crystals were cut to obtain a cross-section of the $ZnAl_2O_4$ layer after impregnation of epoxy resin under a vacuum [14], and polished with 1 μm diamond paste. Natural pores introduced by the growth of the zinc aluminate layer were observed under a dark field

0022-2461/89 $03.00 + .12

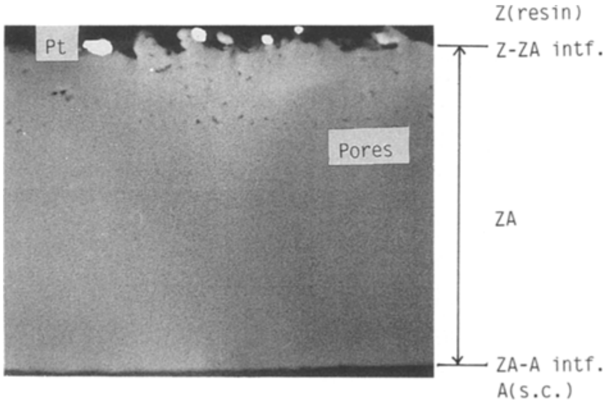

Figure 1 Zinc aluminate layer observed by SEM after polishing (Z, ZnO; A, Al_2O_3; ZA, $ZnAl_2O_4$; Pt, platinum marker).

illumination of an optical microscope. An Hitachi model H-800 electron microscope was used in a scanning mode (SEM), and the cation distribution in the reaction layer was determined with attached energy dispersive X-ray analyser (EDX). The concentration profile of the cations was calculated with KEVEX 8000S.

To observe the grain structure of the reaction layer, thermal etching was carried out as follows. Polished samples were taken out from the mounted epoxy resin after gradual burning up to 600° C, and treated at 1000° C for 1 h avoiding an increase in the thickness of the reaction layer.

3. Results and discussion

3.1. Zinc aluminate layer grown on the surfaces of alumina single crystal

Microstructures of the reaction layer on alumina single crystal were observed by SEM. Fig. 1 shows the cross-sectional view of the layer. Some pores were confirmed in the zinc aluminate layer near to the ZnO–$ZnAl_2O_4$ interface.

The square of the thickness of the zinc aluminate layer was plotted against the heating time for various heating temperatures as shown in Fig. 2. A linear relationship between the square of the spinel layer thickness, x^2, and the heating time, t, was obtained at each heating temperature

$$x^2 = k_{\text{Single crystal}} \cdot t \qquad (1)$$

Fig. 3 shows the concentration profile of zinc in the spinel layer determined by the EDX analyser. An almost linear decrease in the concentration of zinc was observed across the reaction layer.

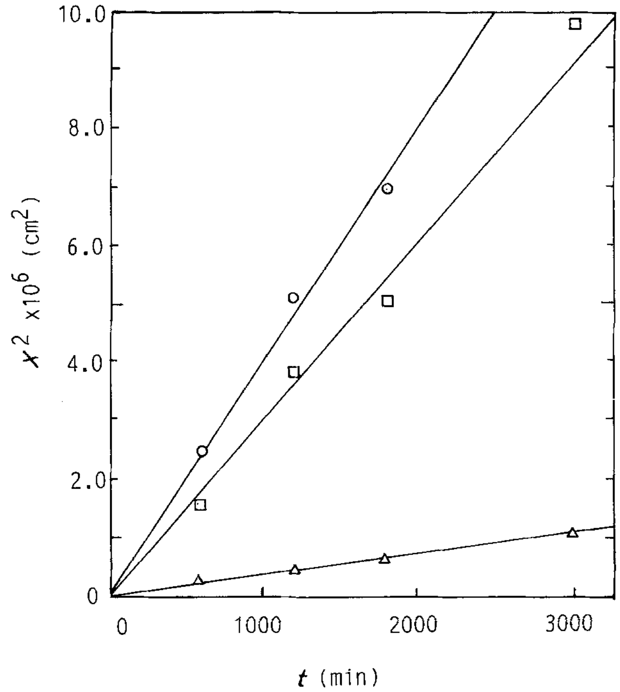

Figure 2 Growth of the thickness of zinc aluminate layer with heating time (○ 1100° C, □ 1300° C, △, 1200° C)

The diffusion controlled mass transport theory was applicable for the present study. One of the solutions of Fick's second law is given by Equation 2 for the diffusion into a semi-infinite solid under the assumption that the diffusion coefficient, D, has no concentration dependence, with the following initial and boundary conditions: for $x = 0, C = C_0$; for $x > 0$, $C = 0$ at $t = 0$ and for $x = 0, C = C_0$ at $t > 0$, [28],

$$C(x, t) = C_0[1 - \mathrm{erf}(x/2\sqrt{D \cdot t})] \qquad (2)$$

The measured reaction layer thickness, x_d, was assumed to be equal to the distance, x, where C in Equation 2 practically falls to zero, being approximated to Equation 3 which satisfies the parabolic relation as Equation 1 [29].

$$x/2\sqrt{D \cdot t} = 3 \qquad (3)$$

Many authors [1–14, 21] assumed the linear

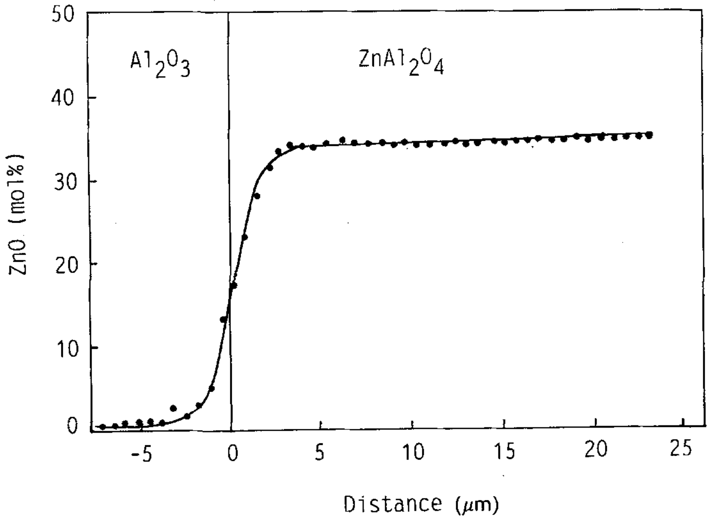

Figure 3 Concentration profile of zinc in zinc aluminate layer grown at 1300° C for 30 h on the surface normal to r axis.

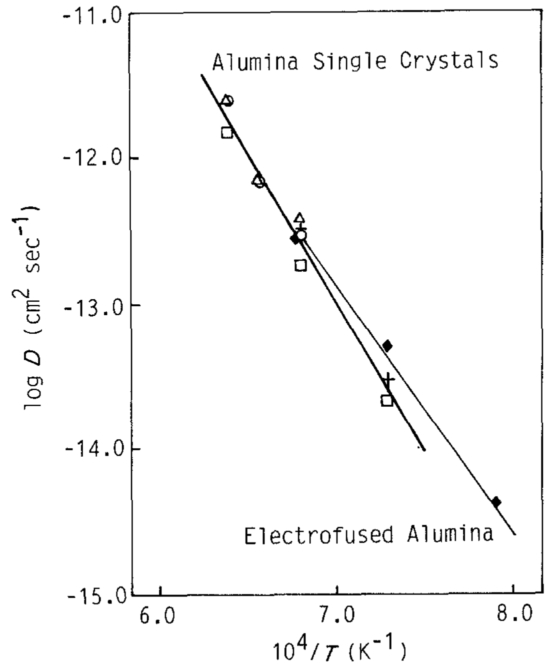

Figure 4 Arrhenius plot of the diffusion constants which control the growth rate of zinc aluminate layer on the surfaces normal to crystal axes of alumina single crystal ○ *c* axis, △ *r* axis, □ *a* axis, ◆ electrofused alumina, + powdered alumina single crystal.

TABLE I Diffusion coefficients controlled the growth of the zinc aluminate layer on the surface normal to the different crystal axes of the alumina single crystal

Temperature (°C)	Diffusion constants (cm^2 sec^{-1})		
	D(a axis)	D(c axis)	D(r axis)
1100	1.98×10^{-14}	2.29×10^{-14}	2.29×10^{-14}
1200	1.75×10^{-13}	2.84×10^{-13}	3.82×10^{-13}
1250	4.90×10^{-13}	6.76×10^{-13}	7.01×10^{-13}
1300	1.41×10^{-12}	2.26×10^{-13}	2.39×10^{-13}
Activation energy of the diffusion (kJ mol^{-1})	385	400	400

distribution of the diffusing species so that the square of the reaction layer thickness was proportional to the reaction time as Jander model [22] and other revised models based on [23–25].

On the other hand, it is possible to make the assumption that the diffusion coefficient depends on the concentration of the diffusing species. The Wagner solution of Fick's second law is applicable in such a case [20]. The linear distribution of the diffusing species in the reaction layer fits to the approximated Wagner solution [30] which assumed the D of a linear function of C and leads to the Equation 4 as discussed elsewhere [14]

$$x^2/2\sqrt{D}\cdot t = 0.81 \qquad (4)$$

The linear distribution of the diffusing species in the reaction layer does not guarantee that the diffusion mechanism is counter diffusion or unidirectional diffusion and is possible for both mechanisms. The square of the reaction layer thickness being proportional to the heating time is, therefore, possible for both mechanisms of diffusion.

By the selection of the equation, we might, however, have different diffusion constants calculated with Equations 3 and 4, but the difference is only a constant factor. During our discussions, we took the former assumption.

3.2. Diffusion which controls the growth rate of the spinel layer

Diffusion constants were, therefore, calculated from Equation 3 with the reaction layer thickness x_d and plotted against the reciprocals of the heating temperatures for the examinations of various surfaces normal to the axes of alumina single crystal as shown in Fig. 4 and tabulated in Table I. Another way to calculate the diffusion constant with the slope, $\Delta C/x_d$, of the concentration of zinc determined by EDX analysis has been tried using Equation 6 obtained by integrating Equation 5 under the assumption of no concentration dependence of the diffusion coefficient and is shown in Table II

$$J = -D\frac{\partial C}{\partial x} = \frac{\varrho}{M}\frac{\partial x}{\partial t} = -D\frac{\Delta C}{x_d} \qquad (5)$$

$$x_d^2 = \frac{2M}{\varrho}D\cdot\Delta C\cdot t \qquad (6)$$

where ϱ is the density of the reaction layer, M the molecular weight of zinc aluminate, J the flux, D the diffusion constant, x_d the reaction layer thickness and t the heating time.

The diffusion constants calculated in different ways agreed well with each other. The activation energies of the diffusion obtained from the Arrhenius plot are shown in Table I. The direction of the crystal axes of the alumina single crystal has no effect on the diffusion rate or on the activation energies. This indicated that the isotropic nature of the diffusion in $ZnAl_2O_4$ formation is similar to the diffusion in magnesia–alumina spinel formation reported by Fulrath [16].

The activation energies obtained in the present study, c.a. 400 kJ mol^{-1}, corresponds to the highest groups of that of the diffusion, determined in the powdered reaction between ZnO and electrofused dense Al_2O_3 [10, 14] and also with that of interstitial diffusion of zinc in spinel solid solution reported by Koumoto *et al.* [31]. They reported the effect of the composition on the diffusion of zinc in $(Zn_xCo_{1-x})O \cdot Al_2O_3$ and $(Zn_xNi_{1-x})O \cdot Al_2O_3$ and concluded that the diffusion of zinc in the spinel layer is governed by the interstitial diffusion mechanism.

It is a reasonable assumption that the interstitial diffusion of zinc ions in the spinel layer is the rate controlling step in the growth of the $ZnAl_2O_4$ layer in dense alumina diffusion couples.

TABLE II Comparison of the diffusion constant controlled the growth of zinc aluminate in the direction of *c* axis of alumina single crystal calculated from Equations 3 and 6

Temperature (°C)	Diffusion constant (cm^2 sec^{-1})	
	Calculated from Equation 3	Calculated from Equation 6
1300	1.20×10^{-12}	1.62×10^{-12}
1400	5.61×10^{-12}	4.93×10^{-12}

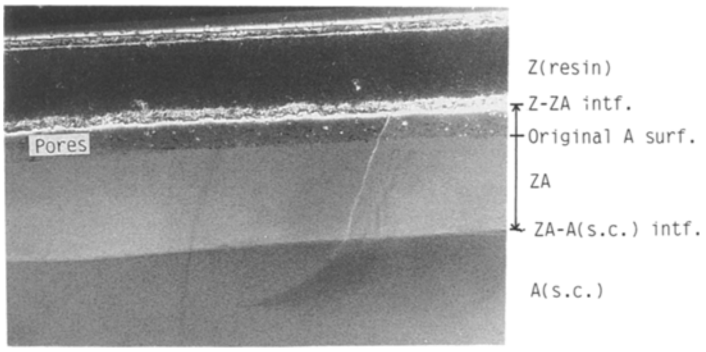

Figure 5 Observation of pores introduced into the zinc aluminate layer near to the zinc oxide–zinc aluminate interface by optical microscope under dark field illumination (Z, ZnO; A, Al_2O_3; ZA, $ZnAl_2O_4$).

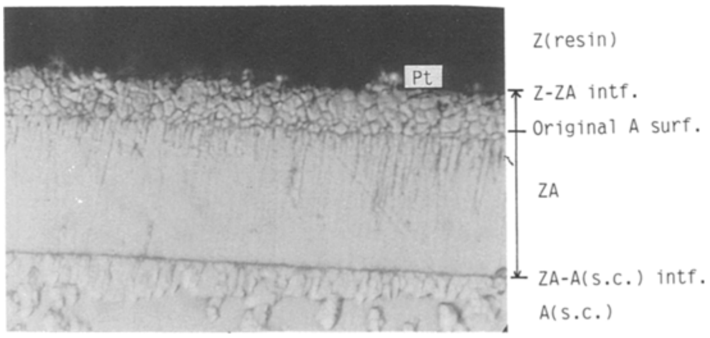

Figure 6 Grain structure of the zinc aluminate grown on the alumina single crystal heated at 1300° C for 50 h and then thermally heated. (Z, ZnO; A, Al_2O_3; ZA, $ZnAl_2O_4$; Pt, platinum marker)

3.3 Grain structure of the $ZnAl_2O_4$ layer grown on an alumina single crystal

The microstructure of the $ZnAl_2O_4$ layer grown on an alumina single crystal indicates the presence of pores in the spinel layer near to the ZnO–$ZnAl_2O_4$ interface.

Fig. 5 shows the microstructure of the reaction layer observed by a dark field illumination using an optical microscope. The photograph shows that the pores are distributed in a quarter of the reaction layer thickness near to the ZnO–$ZnAl_2O_4$ interface.

The result of the thermal etching treatment revealed in Fig. 6 that the area containing many pores has a texture of small grains, and the rest of the reaction layer which corresponded to the three quarters of the reaction layer thickness near the Al_2O_3–$ZnAl_2O_4$ interface shows no grain structure. It should be noticed that an inert marker put on the original surface of alumina single crystal is found at the ZnO–$ZnAl_2O_4$ interface.

Wagner proposed a mechanism of counter diffusion of cations for the diffusional transportation that anions did not move [20]. According to the Wagner theory, the ratio of the product layer thickness grown to the ZnO side to that grown into alumina single crystal is 1/3. Therefore, the original surface of the alumina single crystal is located at a distance of one quarter of the reaction layer from the ZnO–$ZnAl_2O_4$ interface.

The two layers observed of different grain structures supports the Wagner mechanism for the $ZnAl_2O_4$ formation on alumina single crystal. In addition, the inert marker must be moved from the original surface of the alumina single crystal to the ZnO–$ZnAl_2O_4$ interface. The possibility of the movement of the inert marker has already been pointed out [23]. A small inert marker put on the alumina single crystal by evaporation was always found at the front of the $ZnAl_2O_4$ layer growing into the ZnO side. This fact indicates the presence of a strong force to push the marker from the alumina to the zinc oxide. The force would be brought about by the movement of the aluminium ion according to the Wagner mechanism.

References

1. B. BENGSTONE and R. JAGITSCH, *Arkiv, Kemi. Mineral. Geol.* **24** (1947) 1.
2. F. S. STONE and R. J. D. TILLEY, "Reactivity of Solids", edited by G. M. Schwab (Elsevier, Amsterdam, 1965) p. 583.
3. D. L. BRANSON, *J. Amer. Ceram. Soc.* **48** (1965) 591.
4. C. A. DUCKWITZ and H. SCHMALZRIED, *Prog. Vacuum Microbalance Tech.* **1** (1972) 301.
5. S. RAMACHANDRAN, A. BARADARAJAN and M. SATYANARAYANA, *Mater. Sci. Eng.* **20** (1975) 63.
6. T. TSUCHIDA, M. KONDO, R. FURUICHI and T. ISHII, *Nippon Kagaku Kaishi* (1974) 1443.
7. T. TSUCHIDA, R. FURUICHI and T. ISHII, *Z. Anorg. Allgem. Chem.* **415** (1975) 175.
8. T. TSUCHIDA, R. FURUICHI and T. ISHII, *Z. Anorg. Allgem. Chem.* **423** (1976) 180.
9. M. R. ANSEAU, E. CAMBIER and C. LEBRUD, *J. Mater. Sci.* **16** (1981) 1121.
10. Y. FUKUHARA, E. SUZUKI, M. HASHIBA, E. MIURA, Y. NURISHI and T. HIBINO, *Yogyo Kyokai Shi* **91** (1983) 281.
11. K. NAKAYAMA, M. HASHIBA, E. MIURA, Y. NURISHI and T. HIBINO, *ibid.* **88** (1980) 43.
12. H. KAWAKAMI, H. OKADA, M. HASHIBA, E. MIURA, Y. NURISHI and T. HIBINO, *ibid.* **90** (1982) 624.
13. C. YOKOYAMA, H. KAWAKAMI, M. HASHIBA, E. MIURA, Y. NURISHI and T. HIBINO, *ibid* **91** (1983) 525.
14. H. OKADA, H. KAWAKAMI, M. HASHIBA, E. MIURA, Y. NURISHI and T. HIBINO, *J. Amer. Ceram. Soc.* **68** (1985) 58.
15. G. YAMAGUCHI and T. TOKUDA, *Bull. Chem. Soc. Japan* **40** (1967) 843.
16. R. C. ROSSI and R. M. FULRATH, *J. Amer. Ceram. Soc.* **46** (1963) 145.

17. K. HIROTA and W. KOMATSU, *ibid.* **60** (1978) 103.
18. A. MORKEL and H. SCHMALZRIED, *Z. Phys. Chem. N. F., Bd.* **32** (1962) 72.
19. F. S. PETIT, E. H. RANDKLEV and E. J. FELTEN, *J. Amer. Ceram. Soc.* **49** (1966) 199.
20. E. KOCH and C. WAGNER, *Z. Phys. Chem.* **B34** (1936) 317.
21. R. LINDNER, A. AKERSTROM, *Z. Phys. Chem.* **6** (1956) 162.
22. W. JANDER, *Z. Anorg. Allgem. Chem.* **163** (1927) 1.
23. R. E. CARTER, *J. Amer. Ceram. Soc.* **44** (1961) 116.
24. R. E. CARTER, *J. Chem. Phys.* **34** (1961) 2010.
25. A. M. GINSTLING and B. BROUNSTEIN, *J. Appl. Chem. USSR*, (Engl. Trans.) **23** (1950) 1327.
26. W. KOMATSU, "Reactivity of Solids", edited by G. M. Schwab (Elsevier, Amsterdam, 1965) p. 182.
27. G. VALENSI, *Compt. Rend.* **202** (1936) 309.
28. W. JOST, "Diffusion in Solid, Liquid and Gases" (Academic Press, New York, 1969) p. 309.
29. W. D. KINGERY, H. K. BOWEN and D. R. UHLMANN, "Introduction to Ceramics" 2nd edn (Wiley, New York, 1975) p. 224.
30. H. SCHMALZRIED, "Solid State Reactions", 2nd edn (Verlag Chemie, 1981) p. 76, 115 and 116.
31. K. KOUMOTO, T. MATSUBARA, M. TAKATA and H. YANAGIDA, *Bull. Chem. Soc. Japan* **52** (1979) 386.

Received 15 March
and accepted 28 July 1988